Electrochimica Acta 212 (2016) 722–733

Contents lists available at ScienceDirect

Electrochimica Acta

journal homepage: www.elsevier.com/locate/electacta

Voltammetric Sensor Modified by EDTA-immobilized Graphene-like Carbon Nitride Nanosheets: Preparation, Characterization and Selective Determination of Ultra-Trace Pb (II) in Water Samples

Zhenyuan Teng[a,1], Hongying Lv[a,1], Luona Wang[a], Lin Liu[a], Chengyin Wang[a,*], Guoxiu Wang[b]

[a] College of Chemistry and Chemical Engineering, Jiangsu Key Laboratory of Environmental Engineering and Monitoring, Yangzhou University, 180 Si-Wang-Ting Road, Yangzhou, 225002, China
[b] School of Mathematical and Physical Sciences, University of Technology, Sydney, City Campus, Broadway, Sydney, NSW 2007, Australia

ARTICLE INFO

Article history:
Received 25 April 2016
Received in revised form 2 July 2016
Accepted 7 July 2016
Available online 7 July 2016

Keywords:
2D material
carbon nitride
surface functionalization
voltammetric sensor
Pb (II) determination

ABSTRACT

A voltammetric sensor for selective determination of ultra-trace Pb (II) was prepared based on EDTA-immobilized graphene-like carbon nitride nanosheets (EDTA-CN-NS), which has been designed to improve the accumulation performance for Pb (II) onto the electrode surface. The EDTA-CN-NS was prepared through pre-oxidation by $K_2S_2O_8$ and silanization by N-(trimethoxysilylpropyl) ethylene-diamine triacetic acid sodium salt. The crystalline structure, morphology and the added functional groups of EDTA-CN-NS were characterized by XRD, SAED, TEM, STEM mapping and FT-IR, which are quite in accord with the catalysis action in cyclic voltammetry test generated by improved accumulation performance of the immobilized EDTA for Pb (II). The detection limit of EDTA-CN-NS/Nafion modified sensor reached 5.7×10^{-13} mol L^{-1} with two linear ranges from $2.1 \times 10^{-12} \sim 1.3 \times 10^{-9}$ mol L^{-1} and $1.3 \times 10^{-9} \sim 1.7 \times 10^{-6}$ mol L^{-1}. The sensor behaves acceptable immunity from common interferences in Pb (II) determination and was employed for analyzing the Pb (II) concentration in different water samples. This work gives new instructions in designing ultra-high sensitive sensors for determination of heavy metal ions using 2D functional materials.

1. Introduction

As the accumulation of heavy metal elements in the human body is non-biodegradable, the high toxicity of heavy metals becomes persistent in all of the ecological ramifications involved, and passes through food chains to humans [1,2]. Among these metals, lead, the metal largely used as an industrial material, for instance in paint, leaded petrol, cosmetics and batteries [3,4], is regarded as a prevalent toxic metal with non-biodegradability in human body. The toxicity caused by lead is chronic and accumulatively damaging to humans [5]. Although the lowest content of Pb (II) ion in drinkable water was defined by Environmental Protection Agency (EPA) in the US, which refers to 7.2×10^{-10} mol L^{-1}, it is still harmful to children [6]. Several methods based on the inductively coupled plasma-mass spectrometry (ICP-MS) [7], graphite furnace atomic absorption spectrometry (GFAAS) [8], atomic absorption spectrometry [9] and Belousov-Zhabotinskii (B-Z) reaction [10]. These techniques have been widely used in the determination of trace metal ions in water samples. In the past 50 years, voltammetric techniques have shown promising prospect in determination of trace metal because of their aspects, which include rapidity, low cost, easy operation, high sensitivity and easy microminiaturization. Among these electrochemical determination methods, stripping differential pulse voltammetry (DPV) has becoming one of the most attractive electrochemical techniques for sensing ultra-trace heavy metals using various kinds of modified electrodes, which can be attributed to its high sensitivity and selectivity [11].

In past decades, electrodes modified by different chemicals have received considerable attention in enhancing of the sensitivity and sensing linear rage of the electrochemical sensing of Pb (II). Various modifiers, including bismuth [12], PAN-incorporated Nafion [13], organic chelates [14–17], natural clay nano materials [18,19], zeolite [20], silica [21], SiO_2-Al_2O_3 [22], hollow fiber-graphite [23], ion-imprinted polymers [24], organic

* Corresponding author. fax: +86 514 87975244; Tel: +86 514 87888454.
E-mail addresses: wangcy@yzu.edu.cn, yzswcy@qq.com (C. Wang).
[1] Zhenyuan Teng and Hongying Lv contributed equally to this work.

http://dx.doi.org/10.1016/j.electacta.2016.07.036
0013-4686/

chelates immobilized at graphene [25], carbon nanotubes [26–28], antimony [29] and complexing agents such as crown ethers [30,31], penicillamine [32] and peptides [33,34] have already been used in improving the electrochemical performance in the determination of Pb (II). Most of these modifiers have a common feature, about which the accumulation ability of the electrode surface for metal ions was enhanced in aqueous solution, in that the amount of the functional groups is abundant, which could accordingly enhance the intensity of the stripping current of the sensor [11]. However, most of the modifiers mentioned above are highly dispersable [14–17] or toxic [12], and their analytical performance, such as sensitivity, are not high enough, only one research have achieved determination of ultra-trace Pb (II) at picomole level [23], which may restricted their further applications.

Ethylenediaminetetraacetic acid (EDTA) has been recognized as a stable chelate towards heavy metal ions. Many peer studies have successfully immobilized EDTA onto different supporting materials, which enhanced the maximum adsorption capacity of heavy metal ions [35–40]. Therefore, functional groups of EDTA can significantly enhance the accumulation performance for metal ions onto the surface of electrode modifiers, which may increase the intensity of the response current in voltammetric analysis of Pb (II). However, immobilizing EDTA onto different supporting materials to enhance the sensing performance of heavy metal ions is rarely reported.

Recently, two-dimensional (2D) materials have attracted a great deal of attention in the realm of electronics, bio-sensing, catalysis and energy storage [41,42]. Among them, graphene-like carbon nitride nano-sheets (CN-NS), obtained by the exfoliation process including ultrasonic treatment, self-assembly, hydrothermal method and thermal exfoliation, has emerged as a promising candidate in photocatalysis, bio-imagining and fluorescence sensing due to its appropriate band gap, high stability and low cost [43–48]. Moreover, carbon nitride materials modified electrodes have special electrochemical responses to several kinds of analytes [45], especially for Cu (II) [49–51] and Hg (II) [52,53]. Li and co-workers employed exfoliated CN-NS as photoelectrochemical materials in selective sensing of Cu (II), and the limit of detection (LOD) is at $\mu mol\,L^{-1}$ level [49]; Li, Long and co-workers has employed CN-NS as an electrode modifier in voltammetric determination of Hg (II), and the LOD is $1.2 \times 10^{-10}\,mol\,L^{-1}$ [52]; Barman and co-workers prepared a CN-NS modified electrode to determine Hg (II) in aqueous solution with the detection limit $9.1 \times 10^{-11}\,mol\,L^{-1}$ [53]. They mentioned in the interferant investigation section that the current responses of Pb (II) and Cu (II) with $\sim 7 \times 10^{-8}\,mol\,L^{-1}$ could be observed. They thought the enhanced responses is due to the amalgam formation after Hg (II) was reduced on the CN-NS surface. But when Pb (II) and Cu (II) were analyzed individually, their sensitivities decreased significantly [53]. By now, direct determination of Pb (II) based on CN-NS modified electrode has never been reported.

In this work, EDTA has been covalently immobilized onto CN-NS using N-(trimethoxysilylpropyl) ethylene-diamine triacetic acid sodium salt as a coupling reagent, and EDTA-CN-NS as an effectively chelating modifier with excellent dispersibility in aqueous solution was prepared at the first time. The electrochemical response of EDTA-CN-NS for Pb (II) detection was much more significant than that of CN-NS without functionalization, and EDTA-CN-NS is able to be used as a novel electrode material in the preparation of ultra-high sensitive sensor for voltammetric determination of Pb (II) with the LOD $5.7 \times 10^{-13}\,mol\,L^{-1}$. The simultaneous electrochemical detection of Pb (II), Cu (II) and Hg (II) using the EDTA-CN-NS/Nafion/GCE was illustrated as well. The environment-friendly and low-cost modified electrode showed good sensitivity, selectivity, reproductivity and stability, which had been applied to the determination of Pb (II) in real water samples with satisfactory results.

2. Experimental

2.1. Chemicals and reagents

Regents were all analytical grade and used without further purification unless otherwise stated. Concentrated sulfuric acid (H_2SO_4), hydrochloric acid (HCl), potassium persurfate ($K_2S_2O_8$), melamine and other regents were all purchased from Sinopharm Chemical Regent Co., Ltd. N-(trimethoxysilylpropyl) ethylene-diamine triacetic acid sodium salt (EDTA-silane), 35% in water was purchased from Gelest Inc., which was used as a silane functionalization agent. The bulk graphitic carbon nitride (bulk-g-C_3N_4) was synthesized by calcinating melamine [43]. Ultrathin graphene-like carbon nanosheets (CN-NS) was prepared via sonication-exfoliation using bulk-g-C_3N_4 as starting material [44,45]. The ultra-pure water used in all following experiments, whose resistivity is 18.2 MΩ cm at 298.2 K, was prepared by distilling deionized water twice. All of the glassware and plastic beakers were steeped by 10% (v/v) HNO_3 for about 24 hours to prevent the interference of metal ions in the container wall, then the vessels were washed 3 times by the ultra-pure water. The solution of Pb (II) was prepared by dissolving $Pb(Ac)_2{\cdot}3H_2O$ in 10% HAc solutions. The concentration of as-prepared Pb (II) solution was standardized by complexometric titration using EDTA as a complexing agent, which refers to $0.02038\,mol\,L^{-1}$ of Pb (II). The stock solution was diluted in 10% HAc solutions to be $0.001019\,mol\,L^{-1}$ using the standardized solution [6]. The electrolyte phosphate buffer solution (PBS, $0.1\,mol\,L^{-1}$) was prepared by mixing the stock solutions of KH_2PO_4 and K_2HPO_4 and was adjusted to appropriate pH by the addition of NaOH or H_3PO_4 solution at the concentration of $0.1\,mol\,L^{-1}$. The dilution process of Pb (II) was conducted by the PBS presented above, and the diluted Pb (II) solution was stored in the disposable polyethylene tubes. To remove Pb (II) by adsorption onto the container walls, 2.1% (v/v) sulfuric acid solution was added into $Pb(Ac)_2{\cdot}3H_2O$ solution [54].

The environmental water samples were collected our research group from a lake and a river in Jiangsu Province, P. R. C. The contents of Pb in these lake water samples had been detected by inductively coupled plasma mass spectroscopy (ICP-MS) method using an Elan DRC-e inductively coupled plasma mass spectrometer (PerkinElmer, USA) as a standard method.

2.2. Apparatus

Powder X-ray Diffraction (XRD) patterns were performed on a Bruker-D8 ADVANCE diffractometer equipped with Cu Kα radiation (λ = 0.15406 nm). The dispersing of the samples was conducted on a SCIENTZ-1200E ultrasonic cell disruptor (Ningbo Scientz Biotechnology Co. Inc.). High Resolution Transmission Electron microscope (HRTEM), Scanning Transmission Electron Microscope (STEM) and Selected Area Electron Diffraction (SAED) were conducted by a Tecnai G2 F30 S-Twin electron microscopy with an accelerating voltage of 200 kV. Fourier Transform Infrared measurements (FT-IR) were recorded on KBr pellets with a PE Paragon 1000 spectrophotometer. Electrochemical measurements were performed on a CHI 660 electrochemical workstation (Chenhua Instruments Co., Shanghai, China).

2.3. Pre-oxidation of CN-NS

The 0.5 g CN-NS was firstly dissolved in 50 mL concentrate sulfuric acid under constant stirring at a temperature of 273.2 K, then 2 g $K_2S_2O_8$ was dissolved in the mixture with constant stirring

for 30 min. After heating the mixture at a raising rate of temperature of 1 K/min to 303.2 K, the mixture was kept under constant stirring for 15 min. Then, the mixture was cooled down to 273.2 K, and 150 mL ultra-pure water was slowly added into the mixture before adding 25 mL 5% hydrogen peroxide into the mixture under constant stirring. After filtration, the precipitate was washed by 5 mL 6 mol L^{-1} hydrochloric acid solution three times, and was sufficiently washed by ultra-pure water. After being dried in a vacuum oven with the pressure of 66.7 kPa at 303.2 K for 24 h, the pre-oxidized CN-NS was prepared.

2.4. Silanization of pre-oxidized CN-NS

To silanize the CN-NS, 20.0 mg of pre-oxidized CN-NS was placed in a three-neck flask. Then, 50.0 mL of tetrahydrofuran was added into the flask, and the flask was sealed and treated by the ultrasonication at a temperature of 303.2 K for 60 min [55]. Then, 2 mL tetrahydrofuran solution containing 1.0 wt % EDTA-silane was dropped into the suspension, and the suspension was kept under vigorous stirring for half an hour. After adding 1 mL ammonia solution (1 mol L^{-1}), the suspension was acutely stirred for 12 h at 333.2 K. Then, the dilution of the unreacted silane after the silanization reaction completed was conducted by addition of 100 mL methanol. The precipitate was filtered and washed sequentially by methanol, water, and acetone. The complete removal of EDTA-silane was examined by dropping onto the surface of a thin layer chromatography (TLC) plate and then placed in iodine chamber. After which CN-NS treated by silane was dried at 313.2 K with pressure at 66.7 kPa for 24 h in a vacuum oven. The as-prepared silanized CN-NS is named as EDTA-CN-NS in the following experimental sections. The procedures of pre-oxidation and silanization towards CN-NS are displayed in Fig. 1.

2.5. Preparation for the electrode

Before the modification of the glassy carbon electrode, the electrode, whose diametre is 3 mm, was polished with aluminium oxide powders (d = 0.05 μm). Then, the polished electrode was washed by double distilled water and rinsed by piranha solution that was prepared by mixing 30% hydrogen peroxide solution with H_2SO_4 at a volume ratio of 1:3, respectively. After being washed by ultra-pure water and absolute ethanol under ultrasonic treatment, the electrode was cleaned by electrochemical scanning of cyclic voltammetry from −0.50 V to + 1.60 V vs. Ag/AgCl electrode in 0.5 mol L^{-1} sulfuric acid solution for 20 cycles. The as-cleaned GCE was then dried in nitrogen steam.

After which 10 mg of EDTA-CN-NS powder was dissolved into 20 mL 5% Nafion solution in a 50 mL disposable polyethylene centrifuge tube with ultrasound treatment for 2 hours. After dropping 6 μL the EDTA-CN-NS Nafion mixtures onto the as-cleaned GCE, the electrode was dride by nitrogen steam at 298.2 K. Bulk-g-C_3N_4, CN-NS and pre-oxidized CN-NS were mixed with the same Nafion solution, which were selected as modifiers for the preparation of GCEs using the same preparation procedure to study the effects on the electrochemical features caused by the silanization of EDTA. Each modification step should be conducted on the same electrode to guarantee the comparability of the date acquired in electrochemical tests, and the GCE should be clean with ultra-pure water, ethanol and acetone to remove the physical adsorption then dried in a nitrogen steam after each electrochemical measurement.

2.6. Measuring the electrochemical performance of the electrode

Unless any other illustration appeared, all of the electrochemical measurements were conducted at the temperature of 298.2 K in the PBS mentioned in the section of Chemicals and reagents. A conventional three-electrode system was employed for all electrochemical measurements, in which a modified electrode, an Ag/AgCl electrode whose concentration of KCl was 3.5 mol L^{-1} and a platinum plate electrode was respectively served as the working electrode (WE), reference electrode (Ref), and counter electrode (CE). The Nafion modified GCE (Nafion/GCE), the bulk-g-C_3N_4/Nafion modified GCE (bulk-g-C_3N_4/Nafion/GCE), the CN-NS/Nafion modified GCE (CN-NS/Nafion/GCE), the pre-oxidized CN-NS/Nafion modified GCE (pre-oxidized CN-NS/Nafion/GCE) and the EDTA-CN-NS/Nafion modified GCE (EDTA-CN-NS/Nafion/GCE) were prepared and tested by cyclic voltammetry (CV), respectively. CV measurements of the five modified GCEs were performed in the presence of 7.7×10^{-7} mol L^{-1} Pb (II) in the PBS from −1.00 V to 1.00 V at a scan rate of 0.05 V s^{-1}. After adding a certain amount of Pb (II) standard solution in the PBS, DPV measurements were

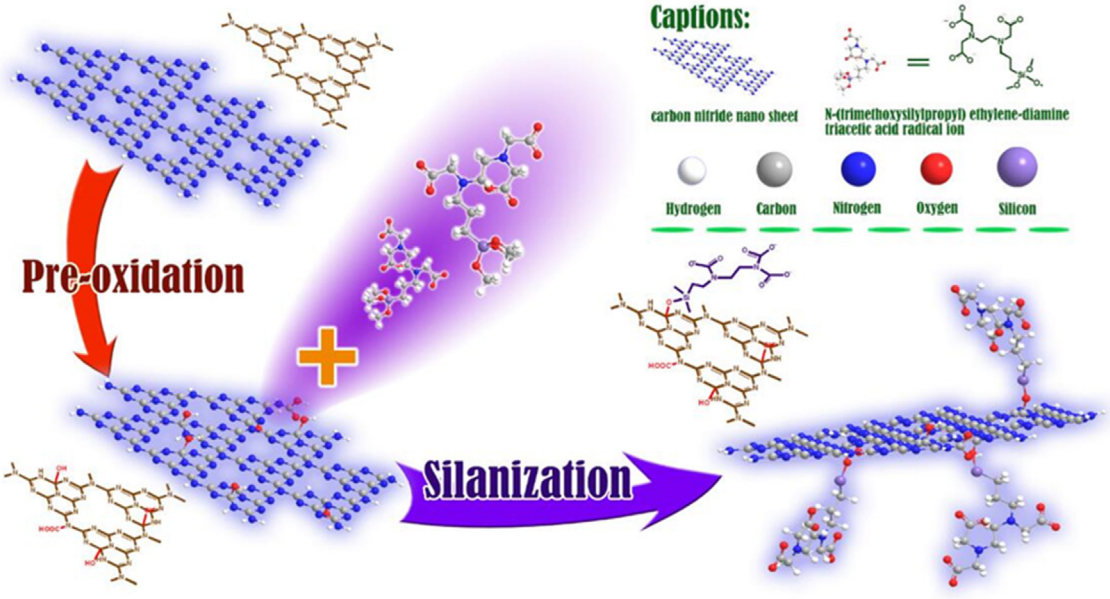

Fig 1. The schematic diagram in the synthesis of EDTA-CN-NS.

conducted by using the same three-electrode system using EDTA-CN-NS/Nafion/GCE as the working electrode from the potential of −0.20 V to + 1.00 V was conducted to examine the sensing performance of the as-prepared electrode towards Pb (II).

The sensor's repeatability was evaluated by testing the intensity of the peak current in DPV measurements. In this experiment, replicate determinations of aqueous solutions containing 2.3×10^{-7} mol L^{-1} Pb (II) were conducted in intra-day and inter-day determinations.

2.7. Solubility and compatibility of EDTA-CN-NS with Nafion in aqueous solution

0.5 g bulk-g-C_3N_4, CN-NS and EDTA-CN-NS were respectively added to 100.0 mL deionized water. Then, these mixtures were dispersed by ultrasonic treatment for 2 hours by an ultrasonic cell disruptor and were poured immediately into three weighing bottles. After being rested for 4 weeks, the solubility of bulk-g-C_3N_4, CN-NS and EDTA-CN-NS was examined by comparing the settlement properties in aqueous solution. The solubility of these three materials in 5% Nafion solution was investigated by the same procedure.

3. Results and discussion

3.1. The dispersibility of EDTA-CN-NS in aqueous solution and its compatibility of Nafion

Fig. 2 shows the flocculation settling velocity of bulk-g-C_3N_4, CN-NS and the EDTA-CN-NS. As shown in Fig. 2a, three kinds of material showed similar dispersibility in aqueous solutions after the ultrasonic treatment. Bulk-g-C_3N_4 showed poor dispersibility in aqueous solution by settling onto the bottom, the CN-NS and EDTA-CN-NS showed good dispersing performance after 48 hours. After resting for 4 weeks, the EDTA-CN-NS formed a well-dispersed suspension in aqueous solution, however, the CN-NS had mostly settled onto the bottom of the bottle, as shown in Fig. 2c. Similar dispersal behaviours in Nafion solution were performed in Fig. 2b and d, as well. Such results indicate a significantly improved dispersibility of EDTA-CN-NS after the silanization in aqueous solution and an acceptable compatibility with Nafion, which may be due to the immobilization of the functional groups, such as EDTA. The silanization of EDTA towards CN-NS may endow possibilities of carbon nitride materials for further applications, for example, the immobilized EDTA may enhance the adsorption capacity of carbon nitrides, which can also serve as a promising functional material for heavy metal adsorption.

3.2. Characterization of EDTA-CN-NS

Fig. 3 shows the XRD patterns of bulk-g-C_3N_4, CN-NS, pre-oxidized CN-NS and EDTA-CN-NS, which reveal the changes in crystal structure through pre-oxidization and silanization process. As shown in Fig. 3a, the diffraction peak of bulk-g-C_3N_4 at 2 θ = 13.1° (d = 0.68 nm) arising from the inter-planar structural packing pattern is indexed as the (100) plane of graphitic carbon nitride, while the strong peak at approximately 2 θ = 27.3° (d = 0.324 nm) is indexed as (002) plane from the inter-layer diffraction of graphitic-like structures. The diffraction pattern of CN-NS shows that the peaks at 27.3° and 13.1° in the diffusion pattern of CN-NS still exists, but both of the 2 peaks have been sharply decreased compared with the peaks in the pattern of bulk-g-C_3N_4, which suggests the few-layered structure of CN-NS [45,49,56–58]. The pattern of the oxidized CN-NS showed similar layer structure like the CN-NS, but the intensity of the peak at 13.1° becomes weaker, which can be due to the simultaneously decrease of the repeated tri-s-triazine structure planar size though the oxidization process. The diffusion pattern of EDTA-CN-NS is quite accordant with oxidized CN-NS, but the intensity of the peak at 27.3° showed a significant decrease, which may be attributed to the a further exfoliation in the crystalline structure the silanization process that caused by the short range disorder of (002) plane in EDTA-CN-NS.

The TEM images of EDTA-CN-NS are shown in Fig. 3b and c, which reveals the morphology of EDTA-CN-NS. As shown in Fig. 3b, it is obvious that the morphology of the nanosheets remained lamellar, and the SAED pattern, which is inserted in Fig. 3c of EDTA-CN-NS, reveals the multicrystalline structure of the g-C_3N_4 [45]. The diffraction ring marked in SADE pattern is quite accord with the interplanar spacing of (002) plane of graphite-like carbon

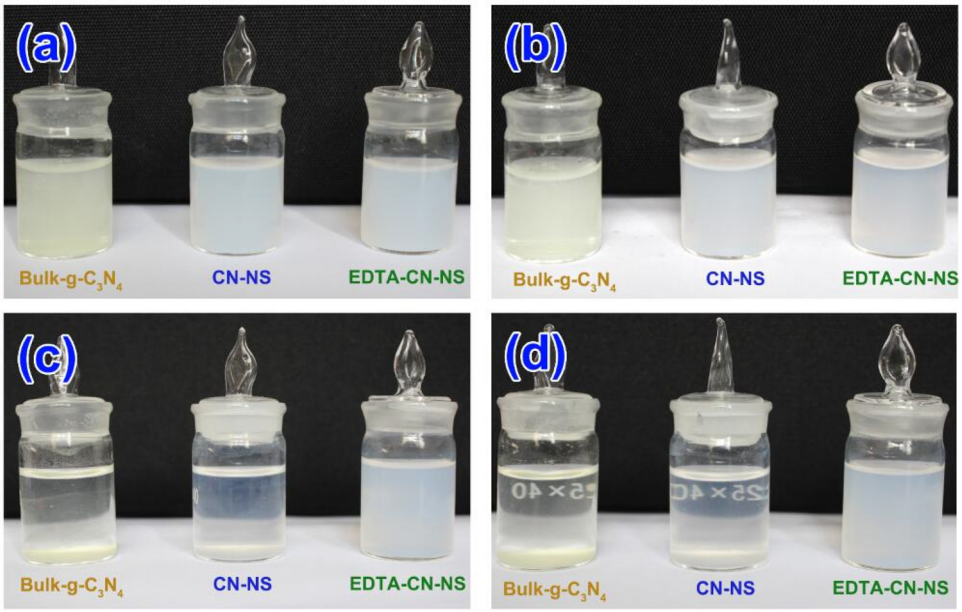

Fig. 2. Digital photos of suspensions containing bulk-g-C_3N_4, CN-NS and EDTA-CN-NS dispersed in deionized water (a) and 5% Nafion solution (b) just after the ultrasonic treatment. Digital photos of suspensions containing bulk-g-C_3N_4, CN-NS and EDTA-CN-NS dispersed in deionized water (c) and 5% Nafion solution (d) resting for 4 weeks.

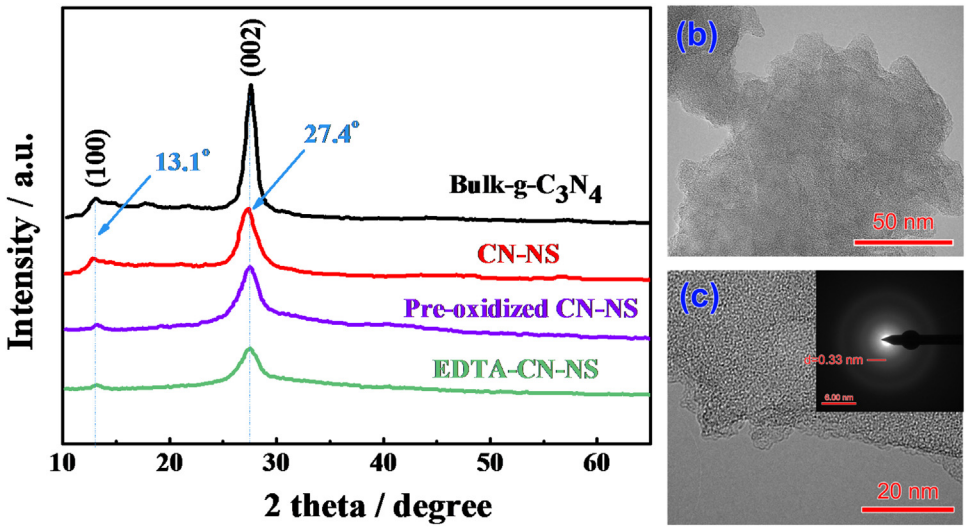

Fig. 3. The influence to the crystal structure and morphology brought from the oxidization and silanization process. XRD analysis of bulk-g-C_3N_4, CN-NS, pre-oxidized CN-NS and EDTA-CN-NS (a). TEM images of the EDTA-CN-NS in different scales (b), (c). The SAED pattern (inserted c).

nitride, which is calculated to be 0.33 nm [59]. Such results reveal that the crystalline structure and monophony of CN-NS still remained after the oxidization and silanization process [45].

The STEM images and the EDS mapping patterns of CN-NS, pre-oxidized CN-NS and EDTA-CN-NS scanning for C, N, O and Si are shown in Fig. 4 to elaborate the changes of the functional groups on the surface of CN-NS. According to the EDS mapping images of the CN-NS and oxidized CN-NS in Fig. 4a and b, the amount of oxygen increases significantly, which is attributed to the oxygen containing groups added onto the surface of the CN-NS during the pre-oxidization process. According to the EDS mapping images of C, N, O and Si obtained during the STEM measurements as shown in Fig. 4c, it is obvious that silicon has been detected by EDS mapping measurement, which indicates the successful silanization.

To further investigate the silanization effects to the functional groups in EDTA-CN-NS, FT-IR spectrum of CN-NS, pre-oxidized CN-NS and EDTA-CN-NS are shown in Fig. 4d, the characteristic absorption peaks of the tri-s-triazine ring and CN heterocycles at 801 cm^{-1} and between 1200 and 1600 cm^{-1} appeals in the FT-IR spectrum of CN-NS and the pre-oxidized CN-NS, which indicates the similar covalent bonds in their structure. Moreover, compared with bulk-g-C_3N_4 and the CN-NS reported in previous literature

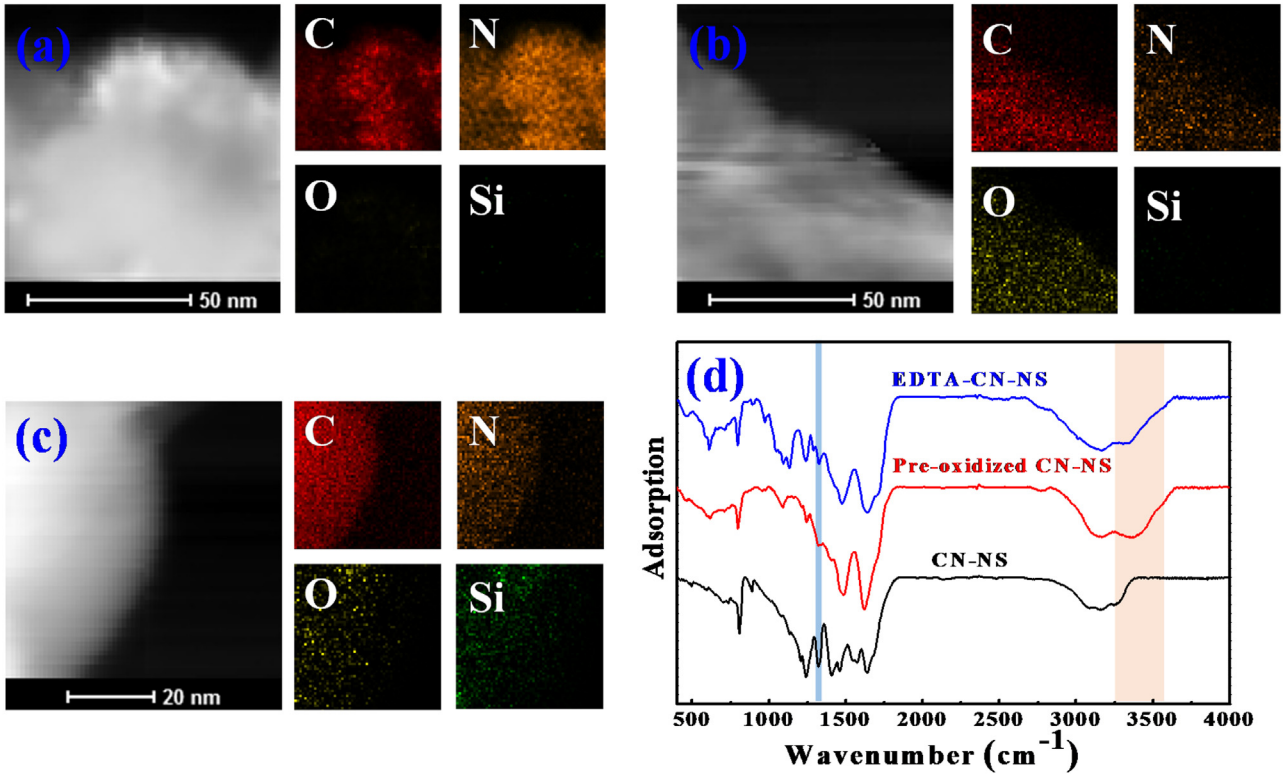

Fig. 4. Effects of the functionalization of CN-NS with N-(trimethoxysilylpropyl) ethylenediamine triacetic acid sodium. The STEM-HAADF image and STEM EDS mapping of CN-NS (a), pre-oxidized CN-NS (b) and EDTA-CN-NS (c). The FT-IR spectrum of CN-NS, pre-oxidized CN-NS and EDTA-CN-NS (d).

[45,49,56,57], the additional absorption peak of pre-oxidized CN-NS at 1088 to 1110 cm-1 revealed the covalent bonds of C-O, and the peaks between 3300 and 3600 cm^{-1} suggest the existence of –OH in the pre-oxidized CN-NS. In addition, the absorption peaks of CN-NS, pre-oxidized CN-NS and EDTA-CN-NS from 1360 to 1310 cm^{-1} and the peaks from 1230 to 1150 cm^{-1} indicates the changing groups of tertiary amine (R_3-N). It reveals, obviously, that the peak intensity of R_3-N shows significant weakening after the pre-oxidation process, which may be attributed to the partial damage of R_3-N caused by $K_2S_2O_8$. However, compared with the absorption peak of R_3-N in pre-oxidized CN-NS, the peak obtained from EDTA-CN-NS showed some degree of enhancement, which may due to the covalent bonds of R_3-N in immobilized EDTA groups. In addition, the adsorption peaks of Si-O between 1110 and 1000 cm^{-1} were obviously detected, which shows that the coupling reagent was successfully bonded with CN-NS. These results from STEM EDS mapping and FT-IR tests clearly show that the functional groups of EDTA were immobilized onto the surface of CN-NS after the process of pre-oxidization and silanization. As EDTA is a well-known chelating agent, EDTA-CN-NS may have great tendency in accumulating heavy metal ions in aqueous solution, which has great potential for preparing ultrahigh sensitive electrochemical sensors in detecting heavy metals.

3.3. Electrochemical behaviours of modified electrodes

Fig. 5 shows the CV characteristics of Nafion (curve a), bulk-g-C_3N_4/Nafion (curve b), CN-NS/Nafion (curve c), pre-oxidized CN-NS/Nafion (curve d) and EDTA-CN-NS/Nafion (curve e) modified GCE in 0.05 mol·L^{-1} PBS (pH 4.5) containing 7.7×10^{-7} mol L^{-1} of Pb (II). Besides, EDTA-CN-NS/Nafion/GCE were tested in PBS (pH 4.5) without Pb (II) (curve f). Compared with the intensity of the current response obtianed from the Nafion/GCE, the intensity of the current response of CN-NS/Nafion/GCE was slightly increased, which suggests weak accumulation effect of CN-NS for heavy metal ions. However, bulk-g-C_3N_4 modified GCE showed extremely weaker intensity of oxidation peak current, which may be attributed to the poor conductivity of the bulk-g-C_3N_4 that hinder the transmission of the charges onto the GCE surface. Moreover, the intensity of the peak currents using CN-NS/Nafion/GCE and Pre-oxidized/Nafion/GCE in the presence of Pb (II) was almost the same, but the potential of the peak current slightly shifted to +0.006 V, which indicates the pre-oxidization process of the CN-NS

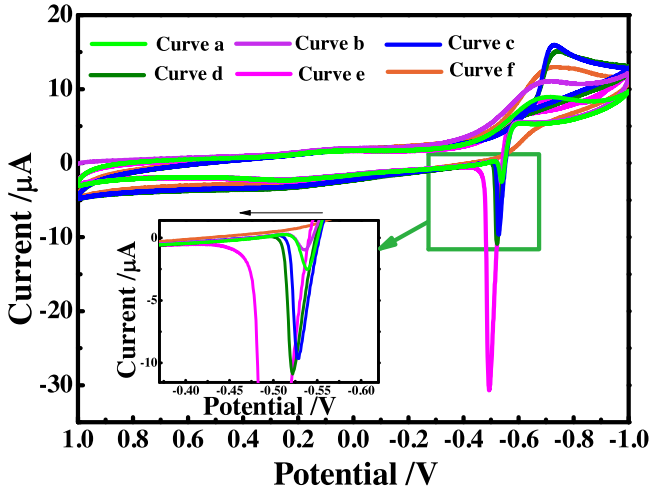

Fig. 5. The CV curves of the Nafion/GCE (curve a), bulk-g-C_3N_4/Nafion/GCE (curve b) CN-NS/Nafion/GCE (curve c), pre-oxidized CN-NS/Nafion/GCE (curve d) and EDTA-CN-NS/Nafion/GCE (curve e) in PBS containing 7.7×10^{-7} mol L^{-1} of Pb (II). The CV curves of the EDTA-CN-NS/Nafion/GCE in blank PBS (curve f).

did not contribute much in its electrochemical performance. In the case of EDTA-CN-NS/Nafion/GCE, a well-defined anodic stripping current peak at the potential of −0.494 V was clearly observed, whose intensity was significantly enhanced. Such results verified that the adsorption ability of electrode surface for Pb (II) ions is greatly enhanced by modification of EDTA-CN-NS, which may significantly enhance the sensor sensitivity. In addition, compared with the equilibrium potential of the Nafion/GCE at −0.527 V, the equilibrium potential of the EDTA-CN-NS/Nafion/GCE shifted + 0.034 V. Such an obvious shift of the potential indicated that EDTA-CN-NS may catalyze the electrochemical reactions on the interface of GCE. Comparing the mechanism in determination of Hg (II) using CN-NS/GCE [53], the electrode reaction equations on the suface of EDTA-CN-NS/Nafion/GCE can be assumed as follows:

Accumulation and reduction step: EDTA-CN-NS/Nafion/GCE (surface) + Pb (II) (solution) +2e^- →EDTA-CN-NS/Nafion/GCE-Pb (0) (surface). (I)

Oxidation step: EDTA-CN-NS/Nafion/GCE-Pb (0) (surface) → EDTA-CN-NS/Nafion/GCE (surface) + Pb (II) (solution) + 2e^-. (II)

To examine these electrochemical reaction mechanisms, CV characteristics should be thoroughly elaborated. According to the Nernst equation, the ideal equilibrium electrode potential of Pb (II)/Pb (vs. Ag/AgCl with 3.5 mol L^{-1} KCl) should be calculated as follows: the standard electrode potential of Pb (II)/Pb (vs. NHE) couple is −0.1262 V, and the equilibrium electrode potential of Ag/AgCl (containing 3.5 mol L^{-1} KCl, vs. NHE) is 0.205 V, thus the standard electrode potential of the Pb (II)/Pb (vs. Ag/AgCl with 3.5 mol L^{-1} KCl) couple equals −0.3312 V; the equilibrium electrode potential of the Pb (II)/Pb couple in the as-mentioned experimental conditions can be calculated using the Nernst equation, which was illustrated as follows:

$$Pb^{2+}(aq) + 2e \rightarrow Pb(s) \quad (1)$$

$$\phi_{Pb^{2+}/Pb} = \phi^{\Theta}_{Pb^{2+}/Pb} - \frac{RT}{zF} ln\left(\frac{a_{Pb^{2+}}}{a_{Pb}}\right) \quad (2)$$

In the as-proposed equation, the perfect gas constant (R) is 8.314 J mol^{-1} K^{-1}, and the temperature of the experiment (T) is 298.2 K, as well as the electron transfer number (z) equals 2, and the Faraday constant (F) is 96485.3383 C mol^{-1} and the standard electrode potential of the Pb (II)/Pb (vs. Ag/AgCl with 3.5 mol L^{-1} KCl) couple ($\Phi_{Pb(II)/Pb}^{\Theta}$) is −0.3312 V. According to the calculation above, because the phase state of the Pb obtained by reduction reaction is solid phase, the a_{Pb} equals 1. After substituting the concentration of Pb (II) into the equation, the equilibrium electrode potential of Pb (II)/Pb (vs. Ag/AgCl with 3.0 mol L^{-1} KCl) equals to −0.512 V. The weak electrochemical features of the Nafion/GCE and CN-NS/Nafion/GCE near −0.527 V were relative to the results of the calculation from the Nernst equation, which suggest that the as-presented assumption is reasonable [60].

The electrochemical mechanism of the potential shift mentioned above can be explained by the as-proposed Nernst equation, R, T, z, F, a_{Pb} and $\Phi^{\Theta}_{Pb(II)/Pb}$ are constants during the CV measurements, the only factor to influence the potential is the activity of Pb (II) ions ($a_{Pb(II)}$) near the surface of the electrode. Compared to the CN-NS/Nafion/GCE, the ennoblement of the equilibrium potential of EDTA-CN-NS/Nafion/GCE reached to + 0.034 V, which refers to the significantly increased $a_{Pb(II)}$ near the surface of the electrode. This phenomenon is most likely due to the pre-oxidation and silanization process that has successfully added some ligands, such as carboxyl, hydroxyl and tertiary amine onto

the surface of the CN-NS, which may effectively chelate the free Pb (II) ions in solution onto the surface of the EDTA-CN-NS/Nafion films modified electrode, and thus, Pb (II) ions in the solution have a much greater tendency to accumulate near the surface of the EDTA-CN-NS/Nafion/GCE than Nafion/GCE and the CN-NS/Nafion/GCE, and therefore, the electrochemical reactions on the interface of the GCE was catalyzed. Additionally, the enhancement of the accumulation ability for Pb (II), which was aroused by the chelation effect of the immobilized EDTA on EDTA-CN-NS, may indirectly increase the intensity of the stripping current.

3.4. Optimization for experimental parameters

The optimal experiments were all conducted in PBS whose content of Pb (II) was 2.3×10^{-7} mol L^{-1}. The current intensity in anodic stripping voltammetric response of the EDTA-CN-NS/Nafion/GCE can be influenced by pH value, which was investigated using PBS at pH value ranging from 3.5 to 6.0. As shown in Fig. 6a, the anodic stripping peak currents kept increasing with continuous enhancing of the pH value at 4.5, then decreased when the pH values increased. The long pair of electrons present on the oxygen and nitrogen atoms may be effected by protonation, and the complexation effect of the active groups on the surface of EDTA-CN-NS such as amidogen, hydroxyl and carboxyl can be weakened accordingly when the pH value is lower than 4.5. The anodic stripping peak currents decreased at the higher pH values, which could be attributed to the hydrolysis reaction of Pb (II). Thus, a pH value of 4.5 was chosen as the optimum pH value for all the subsequent experiments.

Another important influencing factor for electrode accumulation and reduction is the pre-concentration potential in the stripping voltammetry measurement. The optimum deposition potential on anodic stripping peak currents at an accumulation time of 350 s was investigated from −0.2 V to −1.0 V. As shown in Fig. 6b, the anodic stripping peak current increased when the deposition potential increased from −0.2 to −0.6 V, and then decreased when potential turned negative more than −0.6 V. Such tendency can be attributed to the reaction of hydrogen evolution in the PBS (pH 4.5), when the negative value of the deposition potential get larger, the hydrogen evolution will be earier to generate. When the pre-concentration potential become more negative than −0.6 V, the deposition of metal ions on the electrode surface can be influenced by the hydrogen evolution near the electrode surface, and thus, the response of the stripping current was also be influenced. Therefore, −0.6 V was chosen as the deposition potential for Pb (II) in all the subsequent tests.

Pre-concentration time can be another a crucial influencing factor for the intensity of the anodic stripping peak current during the stripping voltammetry measurement. Fig. 6c shows the anodic stripping peak current at several independent deposition times ranging from 50 s to 500 s under the deposition potential of −0.6 V in PBS (pH 4.5). The anodic stripping peak current increased

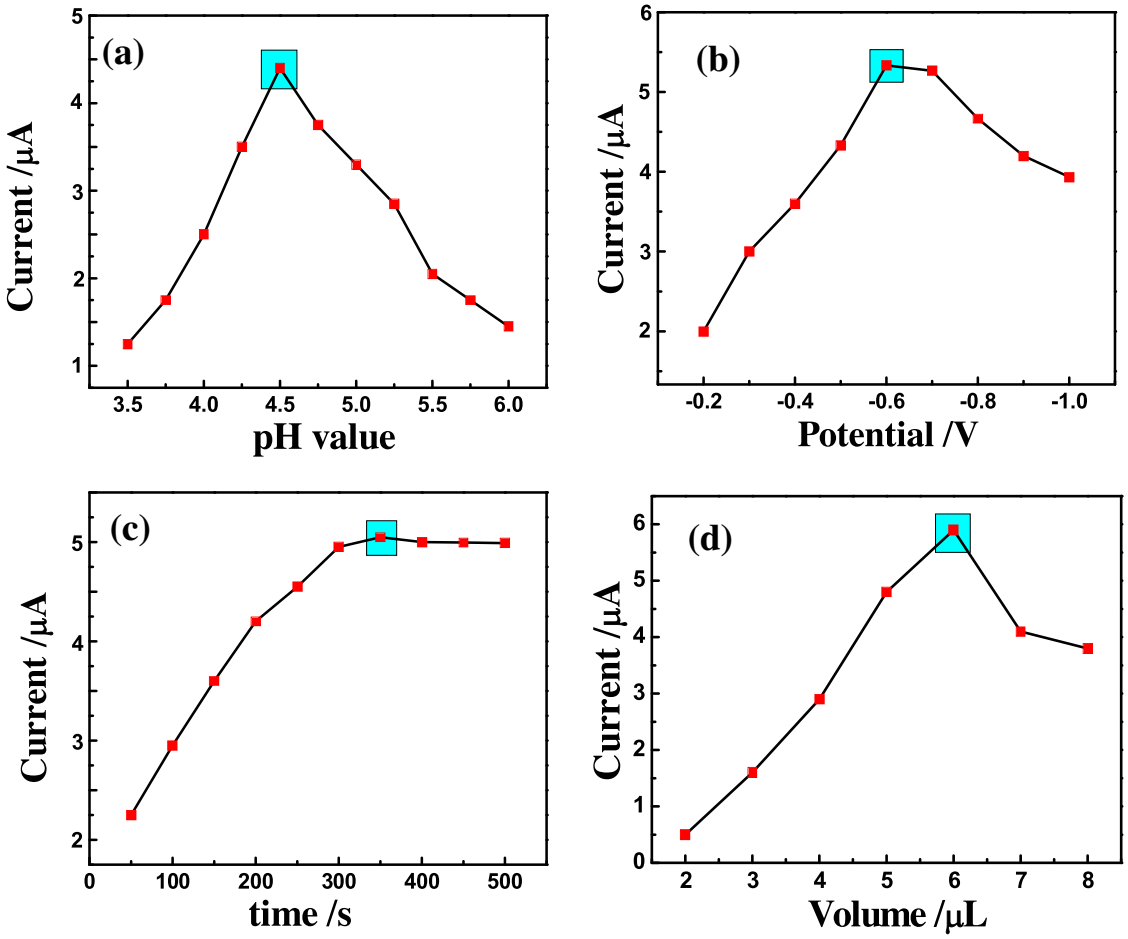

Fig. 6. Optimization of experimental parameters in PBS solution containing 2.3×10^{-7} mol L^{-1} Pb (II) via measuring the peak current of differential pulse anodic stripping in different conditions. (a) Effects of the pH values in the peak current peak intensity applied EDTA-CN-NS/Nafion/GCE. (b) Effect of the pre-concentration potential in the peak current peak intensity applied EDTA-CN-NS/Nafion/GCE. (c) Influence of the pre-concentration time in the peak current peak intensity applied EDTA-CN-NS/Nafion/GCE. (d) Influence of the peak current caused by modifying different volume of EDTA-CN-NS/Nafion suspension onto GCE. Quiet time: 30 s; Scan rate: 0.005 V s^{-1}; Pulse amplitude: 0.050 V; Sampling width: 0.05 s; Pulse period: 0.2 s; Step potential: 0.004 V; Sensitivity: 1.0×10^{-5} A V^{-1}.

linearly with pre-concentration time up to 350 s. When the pre-concentration time was extended, the anodic stripping peak current tended to keep constant due to the saturation loading of active sites at the electrode surface. Therefore, 350 s was selected as the optimum pre-concentration time for all later experiments.

The volume of EDTA-CN-NS/Nafion suspension adding onto the GCE could be another factor during the stripping voltammetry measurement. The EDTA-CN-NS/Nafion suspension at a concentration of 1.0 mg L^{-1} in various volumes ranging from 2 μL to 8 μL were dropped onto the GCE to examine the changes in the intensity of the anodic stripping peak current in a PBS (pH 4.5) ions at a deposition potential of −0.6 V and the pre-concentration time of 350 s, as shown in Fig. 6d. The peak current increased significantly with increasing film thickness before the dropping volume of 6 μL, which was mainly caused by the increased active surface area of EDTA-CN-NS film and the enhanced chelation effect by increased electron donating groups on the EDTA-CN-NS/Nafion film. When the dropping volume of the EDTA-CN-NS/Nafion suspension exceeded 6 μL, the densitiy of the peak current showed slightly decrease, which can be attributed to the excessive thickness of the film. As bulk-g-C_3N_4 has performed extremely poor conductivity, which is presented in Fig. 5, curve b. Therefore, the excessive dropping of the EDTA-CN-NS suspension may increase the thickness of the film, which may weaken the electrical conductivity of the sensor and, accordingly influence the current intensity generated by redox reactions. Therefore, the condition of dropping 6 μL EDTA-CN-NS suspension at a concentration of 1.0 mg L^{-1} onto the suface of the GCE was selected to prepare EDTA-CN-NS/Nafion film in suitable thickness for all subsequent measurements.

3.5. Voltammetric determination of Pb (II)

As the surface of the EDTA-CN-NS was modified by many functional groups, which have a greater tendency for metal ion accumulation. The chelation of EDTA-CN-NS for Pb (II) could increase the amount of the charged particles on the surface of the electrode, which is expected to give a much larger signal change magnitude than other sensors modified by either bulk-g-C_3N_4 or CN-NS. Under optimal conditions, Fig. 7 shows that the DPVs peak currents increased with the increasing concentration of Pb (II) in PBS. Two linear plots of the anodic stripping peak current changes (Δi_p) versus the concentrations of Pb (II) ($C_{Pb(II)}$) in the range of 2.1×10^{-12} mol L^{-1} to 1.3×10^{-9} mol L^{-1} and the range of 1.3×10^{-9} mol L^{-1} to 1.7×10^{-6} mol L^{-1}, and the detection limit is 5.7×10^{-13} mol L^{-1} at a signal to noise ratio of 3. The linear regression equations are inserted in Fig. 7, which are presented follows:

$$\Delta i_p = 0.5694 C_{Pb(II)} + 61.52 \quad (\Delta i_p\text{: nA, } C_{Pb(II)}\text{: pmol L}^{-1}, R^2 = 0.990) \quad (3)$$

$$\Delta i_p = 15.69 C_{Pb(II)} + 2.424 \quad (\Delta i_p\text{: μA, } C_{Pb(II)}\text{: μmol L}^{-1}, R^2 = 0.998) \quad (4)$$

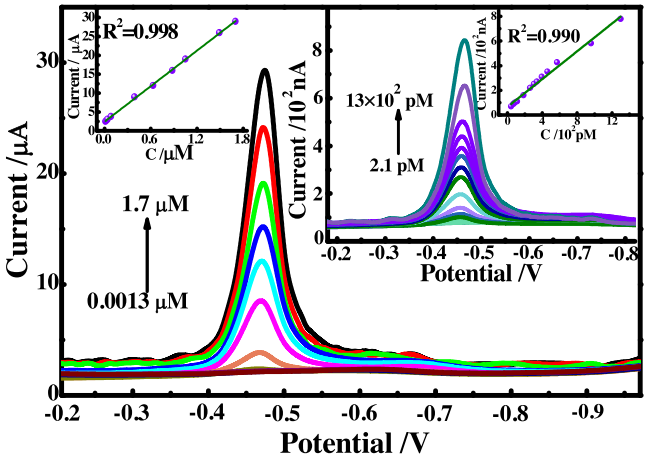

Fig. 7. Linear calibration graphs of EDTA-CN-NS/Nafion/GCE at higher and lower concentrations of Pb (II) under optimized experimental conditions. Accumulation potential under stirring: −0.6 V; Accumulation time: 350 s; Quiet time: 30 s; Scan rate: 0.005 V s^{-1}; Pulse amplitude: 0.05 V; Sampling width: 0.0333 s; Pulse period: 0.2 s; Sensitivity: 1.0×10^{-5} A V^{-1}.

Table 1 compares our analytical method with other voltammetric methods in detecting Pb (II), which indicates that our preparation strategy shows a lower detection limit and wider linear relationship than most of the as-presented analytical methods. Such results can be attributed to the accumulation of Pb (II) onto the surface of the electrode in electrochemical measurements via the chelate effect of the electron donating groups. Although our strategy shows a lower sensitivity than a hollow fiber-graphite electrode [23], the linear relationship of our analytical method can reach to ppb level, which may exhibit more extensive applications in determination of Pb (II) in samples from a variety of sources. Compared with the procedure in preparation of the hollow fiber-graphite electrode [23], the preparation for the hollow fiber and the different kinds of nano materials are not needed in our preparation technique, which demonstrates its simplicity and easy operation. Therefore, our preparation strategy may provide new instructions for design ultra-high sensitive sensors.

3.6. Anti-contamination performance of the EDTA-CN-NS/Nafion/GCE

Anti-contamination ability is also an important factor in evaluating the performance of the sensor. The renewed sensor was prepared by in-situ an electrochemical cleaning process at +0.5 V for 300 s after the first DPV measurement. Obviously no stripping current peak can be observed after the cleaning process in the blank solution, this indicates the complete removal of the accumulated Pb (II). Then, the renewed electrode was used to examine the contamination of the surface of the electrode during the latest test. Fig. 8 shows that the as-prepared electrode was examined by testing the current intensity of the newly modified electrode (curve a1) and the renewed electrode (curve a2 - curve a4) was tested in the solution containing 2.3×10^{-7} mol L^{-1} Pb (II). To ensure the complete removal of Pb (II) on the surface of the electrode, the renewed electrode was examined by DPV method in blank solution (curve b1-curve b4) before the following tests. Applying the same GCE conducted by the same renewed procedure several times, the following curves of the anodic stripping peak currents showed acceptable coincidence with the first curve in the detecting of Pb (II). Additionally, the reproducibility of the current curves in the blank solution also indicated the successfully removal of the Pb (II) from the electrode. These results indicate the excellent anti-contamination ability of the sensor [60]. Then, stability of the EDTA-CN-NS/Nafion GCE at 298.2 K was examined. After 3 months, the as-prepared sensor remained about 92.3% of its initial intensity of the current in the solution containing 2.3×10^{-7} mol L^{-1} Pb (II). As listed in Table 2, the relative standard deviations (RSDs) of the intra-day and inter-day in the peak current of the differential pulse stripping measurements were 1.2% and 1.4%, respectively, which indicates the acceptable repeatability of the method. The evaluation of fabrication reproducibility towards the developed sensor is obtained according to testing 2.3×10^{-7} mol L^{-1} Pb (II) by using five EDTA-CN-NS/Nafion/GCEs based on five GCEs with the same production batch. The RSDs of peak currents were calculated to be 3.2% and 5.2% in intra-day and inter-day determination, respectively, which indicated that the proposed electrode processes good fabrication reproducibility. After three mouths, the average current

Table 1
Comparison of the sensing performance of the as-proposed electrode with other sensors in determination of Pb (II) using voltammetric methods.

Electrode	LOD* ($mol\,L^{-1}$)	Linear range ($mol\,L^{-1}$)	Ref.
PAN/Nafion/GE	1×10^{-8}	5×10^{-8}~1×10^{-5}	[13]
9,10-anthraquinone modified Na-montmorillonite GCE	1×10^{-9}	2×10^{-9}~1×10^{-6}	[14]
TPP-kaolinite/CPE	8.4×10^{-8}	3×10^{-7}~2×10^{-5}	[19]
Zeolite/NH_4-Y/CPE	1.7×10^{-8}	2.5×10^{-8}~1×10^{-7}	[20]
2-benzothiazolethiol/ SBA-15/silica/CPE	4.0×10^{-8}	3.00×10^{-7}~7.00×10^{-6}	[21]
SiO_2-Al_2O_3/CPE	1.07×10^{-9}	2.0×10^{-9} ~5.2×10^{-5}	[22]
HF-GE	9.1×10^{-16}	2.9×10^{-15}~ 4.0×10^{-11}	[23]
IIP-MCPE	3.0×10^{-11}	1.0×10^{-10}~1.0×10^{-8} & 1.0×10^{-8}~1.0×10^{-5}	[24]
HP-β-CD-RGO/Nafion/GCE	9.42×10^{-11}	1×10^{-10}~9×10^{-9}	[25]
TCA-MWCNT/GCE	4×10^{-11}	2×10^{-10}~1×10^{-8}	[26]
Bi-CNT electrode	6.2×10^{-9}	9.7×10^{-9}~4.8×10^{-7}	[27]
BiOCl/MW-CNT/GCE	1.9×10^{-6}	5.0×10^{-6}~5.0×10^{-5}	[28]
CB-18-crown-6-GEC	6.2×10^{-8}	2.1×10^{-8}~1.0×10^{-6}	[30]
CB-15-crown-5-GEC	5.7×10^{-8}	1.9×10^{-8}~1.0×10^{-6}	[30]
4-carboxybenzo-18-crown-6-GEC	7.2×10^{-9}	2.4×10^{-8}~9×10^{-7}	[31]
4-carboxybenzo-15-crown-5-GEC	1.6×10^{-8}	5.2×10^{-8}~9×10^{-7}	[31]
D-penicillamine/aryl diazonium salt monolayers/GCE	1.5×10^{-8}	4.9×10^{-8}~5.6×10^{-7}	[32]
GSH-SPCNFE	1.4×10^{-8}	4.8×10^{-8}~7.2×10^{-7}	[33]
EDTA-CN-NS/Nafion/GCE	5.7×10^{-13}	2.1×10^{-12}~5.7×10^{-10} & 1.3×10^{-9}~1.7×10^{-6}	This method

LOD* means the limit of the detection.

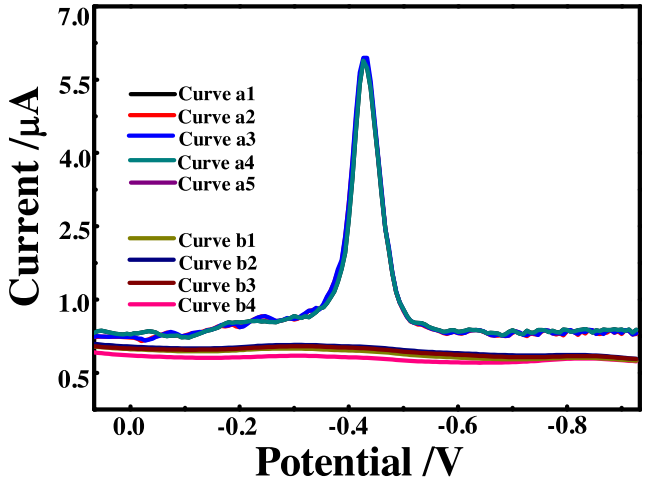

Fig. 8. The differential pulse stripping voltammograms curves of EDTA-CN-NS/Nafion/GCE (curve a1) and the renewed electrode (curve a2 - curve a5) in the solution containing $2.3\times10^{-7}\,mol\,L^{-1}$ Pb (II) and the renewed electrode (curve b1-curve b4) were measured by DPV method in blank PBS. Accumulation potential under stirring: −0.6 V; Accumulation time: 350 s; Quiet time: 30 s; Scan rate: $0.005\,V\,s^{-1}$; Pulse amplitude: 0.05 V; Sampling width: 0.0333 s; Pulse period: 0.2 s; Sensitivity: $1.0\times10^{-5}\,A\,V^{-1}$.

Table 2
Repeatability of the method in detecting $2.3\times10^{-7}\,mol\,L^{-1}$ Pb (II) in aqueous solution by EDTA-CN-NS/Nafion/GCE (n = 5).

Sample	The intensity of the peak current in the DPV measurements	
	Run-to-run (μA)	Day-to-day (μA)
1	6.31	6.21
2	6.21	6.06
3	6.12	6.05
4	6.17	6.27
5	6.03	6.11
RSD	1.5%	1.4%

intensities of these five electrodes remained about 91.2% of its initial intensities for the determination of $2.3\times10^{-7}\,mol\,L^{-1}$ Pb (II), indicating that the durability of the as-prepared sensors is acceptable.

3.7. Interference study

The selectivity of the as-proposed method was investigated as other metal ions might influence the detecting of Pb (II) in real sample analysis. In previous literature, CN-NS showed enhanced electrochemical response in detecting Pb (II) when Hg (II) existed [53], and the chelating constant of EDTA for Hg (II) is much larger than that for Pb (II), so Hg (II) may be the strongest interfering factor in the determination procedure presented above. Hg (II) and some other metal ions have been examined as possible interferents under the optimized Pb (II) detection condition. Fig. 9 shows a DPV

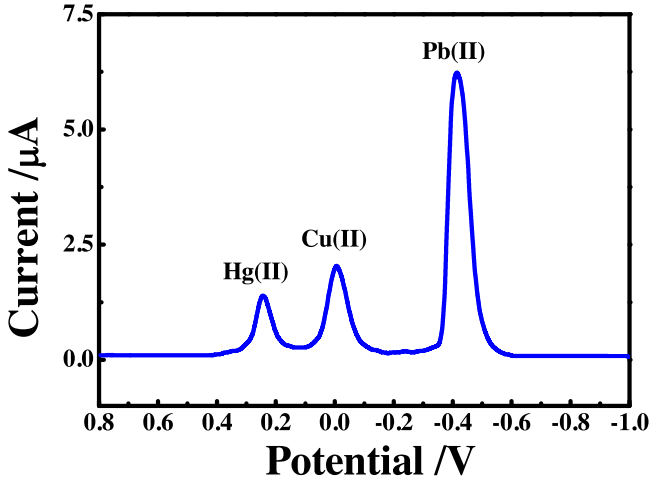

Fig. 9. The DPV voltammograms of $2.3\times10^{-7}\,mol\,L^{-1}$ Pb (II) in presence of $2.3\times10^{-5}\,mol\,L^{-1}$ each of Cu (II), Hg (II), Cd (II), Fe (II), Zn (II), Ni (II) ions at EDTA-CN-NS/Nafion/GCE. Accumulation potential under stirring: −0.6 V; Accumulation time: 350 s; Quiet time: 30 s; Scan rate: $0.005\,V\,s^{-1}$; Pulse amplitude: 0.05 V; Sampling width: 0.0333 s; Pulse period: 0.2 s; Sensitivity: $1.0\times10^{-5}\,A\,V^{-1}$.

voltammogram for the determination of 2.3×10^{-7} mol L^{-1} Pb (II) in presence of some metal ions such as Cu (II), Hg (II), Cd (II), Fe (II), Zn (II), Ni (II) with 2.3×10^{-5} mol L^{-1} content, respectively. It can be seen that sharp stripping peaks due to Hg (II) and Cu (II) also appeared at 0.244 V and −0.001 V, respectively, whereas Zn (II), Cd (II), Ni (II) and Fe (II) have no significant response. Therefore, the simultaneous detection of Cu (II), Hg (II) and Pb (II) was also investigated, as shown in Fig. 10. The peak currents increased linearly with increasing concentration of Cu (II) and Hg (II). The detection limits of Hg (II) and Cu (II) calculated from the calibration curves are found to be 2.7×10^{-7} and 9.0×10^{-8} mol L^{-1}. Both linear ranges of the calibration curves were from 4.3×10^{-7} to 2.1×10^{-6} mol L^{-1} for the determination of Cu (II) and 6.4×10^{-7} to 2.1×10^{-6} mol L^{-1} for that of Hg (II). The existence of plenty interfering ions may still influence the electrochemical response of the target ion in the DPV measurement [24]. Therefore, the stripping peak current voltammograms of 2.3×10^{-7} mol L^{-1} Pb (II) in the presence of different concentrations of Hg (II) need to be examined under optimized conditions. The existence of Hg (II) at an increasing ratio possesses a negligible influence on the electrical signal of Pb (II), and when the excess of Hg (II) reached 75 times the concentrations of Pb (II), the signal of Pb (II) was clearly affected. Such tendency reveals that the competition between Hg (II) and Pb (II) for occupying the chelating sites on the surface of EDTA-CN-NS may play a leading role in reducing the intensity of DPV current in detecting Pb (II), rather than the formation of amalgam with the reduced mercury on the surface of CN-NS. Furthermore, the influence of the peak current of Pb (II) in DPV measurements caused by other interfering ions were listed in Table 3. It can be easily observed that all tested interfering ions had little effects on the intensity of the stripping peak current of Pb (II). The tolerance limit was defined by the maximum concentration of interfering ions that caused a relative error of 5% in the intensity of the current peaks in DPV measurement. It is clear that some interfering ions as possible co-existence ions in environmental water systems, possess no significant effect on the determination of Pb (II), which indicates that EDTA-CN-NS/Nafion/GCE electrode can selectively detect Pb (II) in aqueous solution.

3.8. Real sample analysis

As lead is a high toxic and non-biodegradable element for human, the content of Pb (II) in water source can be regarded as an important indicator to evaluate the safety of drinking water. To examine the potential application in real water sample analysis, the as-prepared sensor was applied to evaluate the lead content in the water samples collected from lake (No. 3) and river (No. 4). Moreover, tap water (No. 1), mineral water (No. 2) and waste water samples (No. 5) were also chosen to examine the performance of the as-prepared electrode in detection of Pb (II) at different concentrations in various real samples. The same procedure was employed for testing the Pb (II) content in same samples without any pre-treatments conducted by ICP-MS. Statistical evaluations of the level of the significance difference were shown in Table 4, in which the calculated t values are all less than the critical value of t (the confidence coefficient 90%), and the relative deviations were in a range from −3.3% to +5.0%. The results of the statistical evaluations indicated that the proposed method showed a good agreement with the ICP-MS. Additionally, the recovery test of Pb (II) was also conducted using sample No. 1, 2 and 4 to present different kinds of water samples containing different contents of Pb (II), as shown in Table 5. The recoveries of Pb (II) from the raw and spiked samples ranged from 97.6% to 105.0%, which reveals the good accuracy of the as-proposed method. Therefore, this method could reliably meet the analytical need for detection of Pb (II) in different water samples.

Table 3
Interference levels for some tested ions in the determination of Pb (II) by EDTA-CN-NS/Nafion/GCE.

Species	Interference level
Cu (II), Hg (II)	>75
Mn (II), Fe (II), Co (II), Ni (II), Zn (II), Cd (II)	>100
Ag (I), Mg (II)	>200
Na (I), K (I), Ca (II),	>1000
NO_3^-, Cl^-, SO_4^{2-}, CO_3^{2-}, PO_4^{3-}, SiO_3^{2-}	>1500

4. Conclusions

In summary, the CN-NS was covalently immobilized by functional groups of EDTA through the pre-oxidization and silanization process. The structure and morphology of EDTA-CN-NS shows no obvious change compared with the CN-NS. It reveals that the EDTA-CN-NS exhibits an excellent dispersibility in aqueous solution, which can form stable suspension for more than 4 weeks. Additionally, the studies of electrochemical performances of the Nafion/GCE, the bulk-g-C_3N_4/Nafion/GCE, the CN-NS/Nafion/GCE and the EDTA-CN-NS/Nafion/GCE reveals that Pb (II) can significantly accumulate onto the surface of the electrode due to the chelating effect of EDTA groups, which

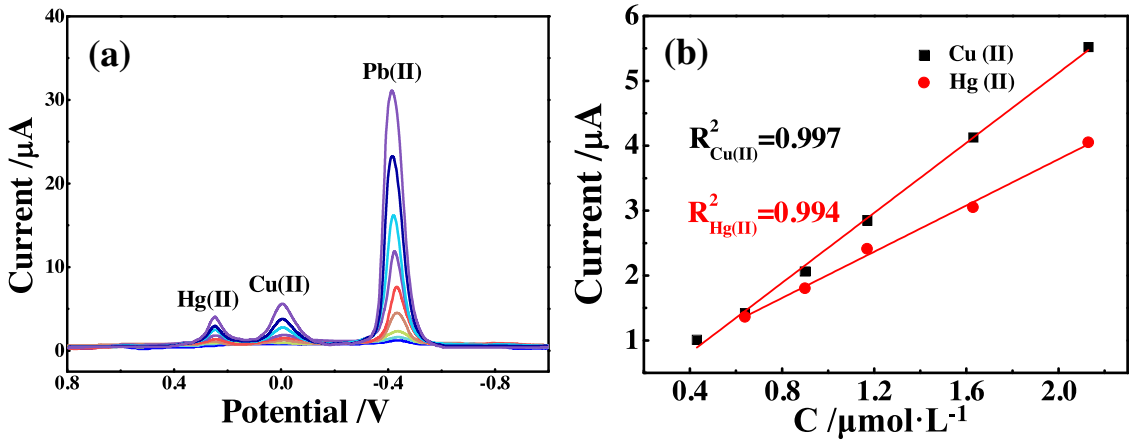

Fig. 10. (a) DPV voltammograms for the different concentrations of Pb (II), Cu (II) and Hg (II) at EDTA-CN-NS/Nafion/GCE, and the concentrations of Pb (II), Cu (II) and Hg (II) in each measurement are all the same. (b) The calibration curve of Hg (II) and Cu (II). Accumulation potential under stirring: −0.6 V; Accumulation time: 350 s; Quiet time: 30 s; Scan rate: 0.005 V s^{-1}; Pulse amplitude: 0.05 V; Sampling width: 0.0333 s; Pulse period: 0.2 s; Sensitivity: 1.0×10^{-5} A V^{-1}.

Table 4
Real water sample testing results and statistical evaluation with a reference method.

Sample numbers	Average found (mol L^{-1}) (n = 5)	Average found by ICP-MS (mol L^{-1}) (n = 5)	Calculated value of t	Critical value of t[a]	Relative deviation (%)
No. 1	4.6×10^{-9}	4.8×10^{-9}	1.76	2.13	−4.2
No. 2	2.1×10^{-11}	2.0×10^{-11}	0.49		5.0
No. 3	3.7×10^{-8}	3.8×10^{-8}	0.21		−2.6
No. 4	2.9×10^{-8}	3.0×10^{-8}	1.26		−3.3
No. 5	7.8×10^{-8}	7.9×10^{-8}	1.13		−1.3

[a] The confidence coefficient 90%.

Table 5
Determination results of Pb (II) in different samples by the EDTA-CN-NS/Nafion/GCE (Number of replicate in each experiment).

Sample numbers	Added (mol L^{-1})	Found (mol L^{-1})	RSD (%)	Recovery (%)
No. 1	–	–	–	–
	4.6×10^{-9}	4.7×10^{-9}	4.2	102.2
	9.2×10^{-9}	9.1×10^{-9}	3.7	98.9
No. 2	–	–	–	–
	2.0×10^{-11}	2.1×10^{-11}	2.9	105.0
	4.1×10^{-11}	4.0×10^{-11}	3.1	97.6
No. 4	–	–	–	–
	2.9×10^{-8}	3.0×10^{-8}	3.3	103.4
	5.8×10^{-8}	5.7×10^{-8}	3.9	98.3

significantly enhanced the intensity of the CV current. An ultra-high sensitive sensor for Pb (II) is proposed. Under the optimized experimental conditions, the EDTA-CN-NS/Nafion/GCE could detect Pb (II) at a concentration of picomole level that reaches 5.7×10^{-13} mol L^{-1} with linear range of $2.1 \times 10^{-12} \sim 1.3 \times 10^{-9}$ mol L^{-1} and $1.3 \times 10^{-9} \sim 1.7 \times 10^{-6}$ mol L^{-1}. The simultaneous electrochemical detection of Pb (II), Cu (II) and Hg (II) using the EDTA-CN-NS/Nafion/GCE was illustrated as well. The resulting studies of interference and real sample analysis showed that EDTA-CN-NS/Nafion/GCE can be used as a highly selective sensor for determination of ultra-trace Pb (II) in water samples.

Acknowledgment

This work was supported by the National Natural Science Foundation of China (Grant Nos. 21375116), a project funded by the Priority Academic Program Development of Jiangsu Higher Education Institutions, and Jiangsu Province research program on analytical methods and techniques on the shared platform of large-scale instruments and equipment (BZ 201409). Results of STEM and XPS in the experiment were provided by Test Center of Yangzhou University.

References

[1] H. Cheng, Y. Hu, Lead (Pb) isotopic fingerprinting and its applications in lead pollution studies in China: a review, Environ. Pollut. 158 (2010) 1134–1146.
[2] H.W. Mielke, M.A.S. Laidlaw, C. Gonzales, Lead (Pb) legacy from vehicle traffic in eight California urbanized areas: Continuing influence of lead dust on children's health, Sci. Total Environ. 408 (2010) 3965–3975.
[3] A. Singh, R.K. Sharma, M. Agrawal, F.M. Marshall, Health risk assessment of heavy metals via dietary intake of foodstuffs from the wastewater irrigated site of a dry tropical area of India, Food Chem. Toxicol. 48 (2010) 611–619.
[4] J.R. Peralta Videa, M.L. Lopez, M. Narayan, G. Saupe, J. Gardea Torresdey, The biochemistry of environmental heavy metal uptake by plants: Implications for the food chain, Int. J. Biochem. Cell Biol. 41 (2009) 1665–1677.
[5] N.C. Papanikolaou, E.G. Hatzidaki, S. Belivanis, G.N. Tzanakakis, A.M. Tsatsakis, Lead toxicity update. A brief review, Med. Sci. Monit. 11 (2005) 329–336.
[6] X. Chen, R. Tian, Q. Zhang, C. Yao, Target-induced electronic switch for ultrasensitive detection of Pb^{2+} based on three dimensionally ordered macroporous Au-Pd bimetallic electrode, Biosens. Bioelectron. 53 (2014) 90–98.
[7] L. Balcaen, L. Moens, F. Vanhaecke, Determination of isotope ratios of metals (and metalloids) by means of inductively coupled plasma-mass spectrometry for provenancing purposes—A review, Spectrochim. Acta Part B 65 B (2010) 769–786.
[8] X. Dong, Y. Nakaguchi, K. Hiraki, Determination of chromium copper, iron, manganese and lead in human hair by graphite furnace atomic absorption spectrometry, Anal. Sci. 14 (1998) 785–789.
[9] M. Camino, M.G. Bagur, M. Sanchez-Vinas, D. Gazquez, R. Romero, Multivariate optimization of solvent extraction of Cd(II), Co(II) Cr(VI), Cu(II), Ni(II), Pb(II) and Zn(II) as dibenzyldithiocarbamates and detection by AAS, J. Anal. At. Spectrom. 16 (2001) 638–642.
[10] J. Gao, H. Chen, H. Dai, D. Lv, J. Ren, L. Wang, W. Yang, Improved sensitivity for transition metal ions by use of sulfide in the Belousov-Zhabotinskii oscillating reaction, Anal. Chim. Acta 571 (2006) 150–155.
[11] M. Zaib, M.M. Athar, A. Saeed, U. Farooq, Electrochemical determination of inorganic mercury and arsenic-a review, Biosens. Bioelectron. 74 (2015) 895–908.
[12] N. Serrano, A. Alberich, J.M. Diaz-Cruz, C. Arino, M. Esteban, Coating methods, modifiers and applications of bismuth screen-printed electrodes TrAC, Trends Anal. Chem. 46 (2013) 15–29.
[13] Z. Hu, C.J. Seliskar, W.R. Heineman, PAN-incorporated Nafion-modified spectroscopic graphite electrodes for voltammetric stripping determination of lead, Anal. Chim. Acta 369 (1998) 93–101.
[14] M.F. Mousavi, A. Rahmani, S.M. Golabi, M. Shamsipur, H. Sharghi, Differential pulse anodic stripping voltammetric determination of lead(II) with a 1,4-bis (prop-2'-enyloxy)-9,10-anthraquinone modified carbon paste electrode, Talanta 55 (2001) 305–312.
[15] C. Hu, K. Wu, X. Dai, S. Hu, Simultaneous determination of lead(II) and cadmium(II) at a diacetyldioxime modified carbon paste electrode by differential pulse stripping voltammetry, Talanta 60 (2003) 17–24.
[16] K. Wagner, J.W. Strojek, K. Koziel, Processes during anodic stripping voltammetry determination of lead in the presence of copper on a solid electrode modified with 2,2'-bipyridyl in polyaniline, Anal Chim. Acta 447 (2001) 11–21.
[17] K.C. Honeychurch, J.P. Hart, D.C. Cowell, Voltammetric studies of lead at a 1-(2-pyridylazo)-2-naphthol modified screen-printed carbon electrode and its trace determination in water by stripping voltammetry, Anal. Chim. Acta 431 (2001) 89–99.
[18] S. Yuan, W. Chen, S. Hu, Simultaneous determination of cadmium(II) and lead (II) with clay nanoparticles and anthraquinone complexly modified glassy carbon electrode, Talanta 64 (2004) 922–928.
[19] Y. Gomez, L. Fernandez, C. Borras, J. Mostany, B. Scharifker, Characterization of a carbon paste electrode modified with tripolyphosphate-modified kaolinite clay for the detection of lead, Talanta 85 (2011) 1357–1363.
[20] S. Senthilkumar, R. Saraswathi, Electrochemical sensing of cadmium and lead ions at zeolite-modified electrodes: Optimization and field measurements, Sens. Actuators B 141 (2009) 65–75.
[21] I. Cesarino, G. Marino, J.d.R. Matos, E.T.G. Cavalheiro, Evaluation of a carbon paste electrode modified with organofunctionalised SBA-15 nanostructured silica in the simultaneous determination of divalent lead, copper and mercury ions, Talanta 75 (2008) 15–21.
[22] M. Ghiaci, B. Rezaei, R.J. Kalbasi, Highly selective SiO_2-Al_2O_3 mixed-oxide modified carbon paste electrode for anodic stripping voltammetric determination of Pb(II), Talanta 73 (2007) 37–45.
[23] Z. Es'haghi, T. Heidari, E. Mazloomi, In situ pre-concentration and voltammetric determination of trace lead and cadmium by a novel ionic liquid mediated hollow fiber-graphite electrode and design of experiments via Taguchi method, Electrochim. Acta 147 (2014) 279–287.
[24] M.K. Bojdi, M.H. Mashhadizadeh, M. Behbahani, A. Farahani, S.S.H. Davarani, A. Bagheri, Synthesis, characterization and application of novel lead imprinted polymer nanoparticles as a high selective electrochemical sensor for ultra-trace determination of lead ions in complex matrixes, Electrochim. Acta 136 (2014) 59–65.
[25] M. Lv, X. Wang, J. Li, X. Yang, C.a. Zhang, J. Yang, H. Hu, Cyclodextrin-reduced graphene oxide hybrid nanosheets for the simultaneous determination of lead (II) and cadmium (II) using square wave anodic stripping voltammetry, Electrochim. Acta 108 (2013) 412–420.
[26] L. Wang, X. Wang, G. Shi, C. Peng, Y. Ding, Thiacalixarene covalently functionalized multiwalled carbon nanotubes as chemically modified electrode material for detection of ultratrace Pb^{2+} ions, Anal. Chem. 84 (2012) 10560–10567.

[27] G.H. Hwang, W.K. Han, J.S. Park, S.G. Kang, Determination of trace metals by anodic stripping voltammetry using a bismuth-modified carbon nanotube electrode, Talanta 76 (2008) 301–308.
[28] S. Cerovac, V. Guzsvany, Z. Konya, A.M. Ashrafi, I. Svancara, S. Roncevic, A. Kukovecz, B. Dalmacija, K. Vytras, Trace level voltammetric determination of lead and cadmium in sediment pore water by a bismuth-oxychloride particle-multiwalled carbon nanotube composite modified glassy carbon electrode, Talanta 134 (2015) 640–649.
[29] N. Serrano, J.M. Diaz-Cruz, C. Arino, M. Esteban, Antimony-based electrodes for analytical determinations, TrAC Trends Anal. Chem. 77 (2016) 203–213.
[30] A. Gonzalez-Calabuig, D. Guerrero, N. Serrano, M. del Valle, Simultaneous Voltammetric Determination of Heavy Metals by Use of Crown Ether-modified Electrodes and Chemometrics, Electroanalysis 28 (2016) 663–670.
[31] N. Serrano, A. Gonzalez-Calabuig, M. del Valle, Crown ether-modified electrodes for the simultaneous stripping voltammetric determination of Cd (II), Pb (II) and Cu (II), Talanta 138 (2015) 130–137.
[32] C. Perez-Rafols, N. Serrano, J. Manuel Diaz-Cruz, C. Arino, M. Esteban, Penicillamine-modified sensor for the voltammetric determination of Cd (II) and Pb(II) ions in natural samples, Talanta 144 (2015) 569–573.
[33] C. Perez-Rafols, N. Serrano, J.M. Diaz-Cruz, C. Arino, M. Esteban, Glutathione modified screen-printed carbon nanofiber electrode for the voltammetric determination of metal ions in natural samples, Talanta 155 (2016) 8–13.
[34] N. Serrano, B. Prieto-Simon, X. Ceto, M. del Valle, Array of peptide-modified electrodes for the simultaneous determination of Pb (II), Cd (II) and Zn (II), Talanta 125 (2014) 159–166.
[35] Y. Zhang, Y. Li, L. Yang, X. Ma, L. Wang, Z. Ye, Characterization and adsorption mechanism of Zn^{2+} removal by PVA/EDTA resin in polluted water, J. Hazard. Mater. 178 (2010) 1046–1054.
[36] L. Yang, Y. Li, L. Wang, Y. Zhang, X. Ma, Z. Ye, Preparation and adsorption performance of a novel bipolar PS-EDTA resin in aqueous phase, J. Hazard. Mater. 180 (2010) 98–105.
[37] E. Repo, L. Malinen, R. Koivula, R. Harjula, M. Sillanpaeae, Capture of Co (II) from its aqueous EDTA-chelate by DTPA-modified silica gel and chitosan, J. Hazard. Mater. 187 (2011) 122–132.
[38] E. Repo, J.K. Warchol, A. Bhatnagar, M. Sillanpaeae, Heavy metals adsorption by novel EDTA-modified chitosan-silica hybrid materials, J. Colloid Interface Sci. 358 (2011) 261–267.
[39] E. Repo, J.K. Warchol, T.A. Kurniawan, M. Sillanpaeae, Adsorption of Co (II) and Ni(II) by EDTA- and/or DTPA-modified chitosan: Kinetic and equilibrium modeling, Chem. Eng. J. 161 (2010) 73–82.
[40] C.J. Madadrang, H.Y. Kim, G. Gao, N. Wang, J. Zhu, H. Feng, M. Gorring, M.L. Kasner, S. Hou, Adsorption behavior of EDTA-graphene oxide for Pb (II) removal, ACS Appl. Mater. Interfaces 4 (2012) 1186–1193.
[41] S.Z. Butler, S.M. Hollen, L. Cao, Y. Cui, J.A. Gupta, H.R. Gutierrez, T.F. Heinz, S.S. Hong, J. Huang, A.F. Ismach, E. Johnston-Halperin, M. Kuno, V.V. Plashnitsa, R.D. Robinson, R.S. Ruoff, S. Salahuddin, J. Shan, L. Shi, M.G. Spencer, M. Terrones, W. Windl, J.E. Goldberger, Progress, challenges, and opportunities in two-dimensional materials beyond graphene, ACS Nano 7 (2013) 2898–2926.
[42] F. Bonaccorso, L. Colombo, G. Yu, M. Stoller, V. Tozzini, A.C. Ferrari, R.S. Ruoff, V. Pellegrini, 2D materials. Graphene, related two-dimensional crystals, and hybrid systems for energy conversion and storage, Science 347 (2015) 1246501.
[43] Y. Zheng, L. Lin, B. Wang, X. Wang, Graphitic carbon nitride polymers toward sustainable photoredox catalysis, Angew. Chem. Int. Ed. 54 (2015) 12868–12884.
[44] J. Zhang, Y. Chen, X. Wang, Two-dimensional covalent carbon nitride nanosheets: synthesis, functionalization, and applications, Energy Environ. Sci. 8 (2015) 3092–3108.
[45] T.Y. Ma, Y. Tang, S. Dai, S.Z. Qiao, Proton-functionalized two-dimensional graphitic carbon nitride nanosheet: an excellent metal-/label-free biosensing platform, Small 10 (2014) 2382–2389.
[46] Y. Zhang, T. Mori, L. Niu, J. Ye, Non-covalent doping of graphitic carbon nitride polymer with graphene: controlled electronic structure and enhanced optoelectronic conversion, Energy & Environmental Science 4 (2011) 4517–4521.
[47] Y. Zhang, T. Mori, J. Ye, M. Antonietti, Phosphorus-doped carbon nitride solid: enhanced electrical conductivity and photocurrent generation, J. Am. Chem. Soc. 132 (2010) 6294–6295.
[48] Y. Zhang, A. Thomas, M. Antonietti, X. Wang, Activation of carbon nitride solids by protonation: morphology changes, enhanced ionic conductivity, and photoconduction experiments, J. Am. Chem. Soc. 131 (2009) 50–51.
[49] X. She, H. Xu, Y. Xu, J. Yan, J. Xia, L. Xu, Y. Song, Y. Jiang, Q. Zhang, H. Li, Exfoliated graphene-like carbon nitride in organic solvents: enhanced photocatalytic activity and highly selective and sensitive sensor for the detection of trace amounts of Cu^{2+}, J. Mater. Chem. A 2 (2014) 2563–2570.
[50] C. Cheng, Y. Huang, X. Tian, B. Zheng, Y. Li, H. Yuan, D. Xiao, S. Xie, M.M.F. Choi, Electrogenerated chemiluminescence behavior of graphite-like carbon nitride and its application in selective sensing Cu^{2+}, Anal. Chem. 84 (2012) 4754–4759.
[51] J. Tian, Q. Liu, A.M. Asiri, A.O. Al-Youbi, X. Sun, Ultrathin graphitic carbon nitride nanosheet: a highly efficient fluorosensor for rapid ultrasensitive detection of Cu^{2+}, Anal. Chem. 85 (2013) 5595–5599.
[52] J. Zhang, Z. Zhu, J. Di, Y. Long, W. Li, Y. Tu, A sensitive sensor for trace Hg^{2+} determination based on ultrathin g-C3N4 modified glassy carbon electrode, Electrochim. Acta 186 (2015) 192–200.
[53] M. Sadhukhan, S. Barman, Bottom-up fabrication of two-dimensional carbon nitride and highly sensitive electrochemical sensors for mercuric ions, J. Mater. Chem. A 1 (2013) 2752–2756.
[54] S. Qiu, L. Xie, S. Gao, Q. Liu, Z. Lin, B. Qiu, G. Chen, Determination of copper (II) in the dairy product by an electrochemical sensor based on click chemistry, Anal. Chim. Acta 707 (2011) 57–61.
[55] S. Hou, M.L. Kasner, S. Su, K. Patel, R. Cuellari, Highly sensitive and selective dopamine biosensor fabricated with silanized graphene, J. Phys. Chem. C 114 (2010) 14915–14921.
[56] P. Niu, L. Zhang, G. Liu, H. Cheng, Graphene-like carbon nitride nanosheets for improved photocatalytic activities, Adv. Funct. Mater. 22 (2012) 4763–4770.
[57] S. Yang, Y. Gong, J. Zhang, L. Zhan, L. Ma, Z. Fang, R. Vajtai, X. Wang, P.M. Ajayan, Exfoliated graphitic carbon nitride nanosheets as efficient catalysts for hydrogen evolution under visible light, Adv. Mater. 25 (2013) 2452–2456.
[58] X. Zhang, X. Xie, H. Wang, J. Zhang, B. Pan, Y. Xie, Enhanced photoresponsive ultrathin graphitic-phase C3N4 nanosheets for bioimaging, J. Am. Chem. Soc. 135 (2013) 18–21.
[59] Y. Huang, Y. Wang, Y. Bi, J. Jin, M.F. Ehsan, M. Fu, T. He, Preparation of 2D hydroxyl-rich carbon nitride nanosheets for photocatalytic reduction of CO_2, RSC Adv. 5 (2015) 33254–33261.
[60] X. Dai, F. Qiu, X. Zhou, Y. Long, W. Li, Y. Tu, Amino-functionalized mesoporous silica modified glassy carbon electrode for ultra-trace copper (II) determination, Anal. Chim. Acta 848 (2014) 25–31.